Estuaries and Coasts: J CERF (2008) 31:402–418
DOI 10.1007/s12237-008-9035-x

Environmental Factors Contributing to the Development and Demise of a Toxic Dinoflagellate (*Karlodinium veneficum*) Bloom in a Shallow, Eutrophic, Lagoonal Estuary

Nathan S. Hall · R. Wayne Litaker · Elizabeth Fensin · Jason E. Adolf · Holly A. Bowers · Allen R. Place · Hans W. Paerl

Received: 17 July 2007 / Revised: 29 November 2007 / Accepted: 11 January 2008 / Published online: 15 February 2008

Abstract A dense bloom of the ichthyotoxic dinoflagellate *Karlodinium veneficum* was discovered in the Neuse River Estuary, North Carolina, on 19 October 2006 and was associated with four subsequent fish kills. Microscopic, photopigment, DNA, and toxicological techniques confirmed bloom identity and toxicity. High-resolution spatio-temporal data from ship-board and fixed automated sampling stations provided a unique opportunity to investigate the environmental conditions that initiated, maintained, and terminated the *K. veneficum* bloom. Bloom initiation and growth were favored by high nutrient availability and reduced dispersal during the period of declining riverine discharge after Tropical Storm Ernesto. *K. veneficum* out-competed other co-occurring dinoflagellates, perhaps because of the production of karlotoxins that are known to act as grazing deterrents and to facilitate mixotrophic feeding. Once the bloom was established, small-scale hydrodynamic processes, coupled with vertical migration, concentrated cells along a frontal convergence to high densities (>200,000 cells per milliliter). By 26 October 2006, wind mixing and possible nutrient stress disrupted the bloom. Release of cell-bound toxins during the bloom collapse likely accounted for the associated fish kill events where fish were reported as exhibiting typical symptoms of karlotoxin poisoning. The dynamics of this bloom underscore the tight control of harmful algal blooms by meteorological forcing, hydrology, and sediment nutrient input in this shallow lagoonal estuary.

Keywords Harmful algal bloom · Dinoflagellate · *Karlodinium veneficum* · Toxin · Fish kill

N. S. Hall (✉) · H. W. Paerl
Institute of Marine Sciences,
University of North Carolina at Chapel Hill,
Morehead City, NC 28557, USA
e-mail: nshall@email.unc.edu

H. W. Paerl
e-mail: hpaerl@email.unc.edu

R. W. Litaker
National Oceanographic and Atmospheric Administration/
National Ocean Service, Beaufort Laboratory,
Beaufort, NC 28516, USA
e-mail: wayne.litaker@noaa.gov

E. Fensin
Environmental Sciences Section,
North Carolina Division of Water Quality,
Raleigh, NC 27699-1621, USA
e-mail: elizabeth.fensin@ncmail.net

J. E. Adolf · H. A. Bowers · A. R. Place
Center of Marine Biotechnology,
University of Maryland Biotechnology Institute,
Baltimore, MD 21202, USA

J. E. Adolf
e-mail: adolf@umbi.umd.edu

H. A. Bowers
e-mail: bowers@umbi.umd.edu

A. R. Place
e-mail: place@umbi.umd.edu

Introduction

Estuarine and coastal phytoplankton blooms commonly result from a sequence of events involving nutrient inputs that stimulate growth and hydrodynamic conditions that favor reduced dispersal or physical accumulation of algal cells. In certain instances, the blooms become dominated by

harmful algal bloom (HAB) species that adversely affect ecosystem or human health. The success of HAB species and their ability to attain bloom concentrations generally result from one or more of the following characteristics: (1) superior ability to utilize or access available nutrients (Amano et al. 1998; Sunda et al. 2006), (2) inhibition of competing phytoplankton through release of allelopathic compounds or direct mixotrophic consumption of competitors (Smayda 1997), (3) reduced grazing losses because of direct toxicity, poor food quality, or mechanical disruption of grazing (Sunda et al. 2006).

On 19 October 2006, a dense dinoflagellate bloom was discovered in the Neuse River Estuary (NRE), North Carolina, USA, by the Neuse River Modeling and Monitoring Program (ModMon; http://www.unc.edu/ims/neuse/modmon/). Morphological, toxicological, pigment, and DNA analyses definitively identified the bloom forming dinoflagellate as *K. veneficum* (see Daugbjerg et al. 2000 for synonyms). *K. veneficum* is common to brackish waters of the US Atlantic Coast and can produce dense "mahogany tides" with cell concentrations approaching 10^6 per milliliter (Goshorn et al. 2004). Fish kills associated with the toxins released by this organism have been reported in estuaries, brackish ponds, and aquaculture systems along the US Atlantic Coast (Deeds et al. 2002; Kempton et al. 2002). In North Carolina estuaries, *K. veneficum* blooms are rare, but background levels <5,000 cells per milliliter are common, particularly during warmer months (Fensin 2004). When *K. veneficum* blooms have exceeded 30,000 cells per milliliter in North Carolina estuaries, they have been associated with fish kills (Fensin 2004). However, definitive attribution of these kills to *K. veneficum* was not possible because the karlotoxin concentration in the water was not measured.

Using a combination of high-resolution data from shipboard sampling and from automated water quality and meteorological monitoring stations, it was possible to investigate the sequence of environmental events and conditions that initiated, supported, and then terminated the October 2006 *K. veneficum* bloom. Of primary interest was how the hydrology of the estuary interacted with nutrient delivery and biological processes to produce the unusually high density of *K. veneficum* cells. This is of importance because a firm understanding of HAB dynamics is required to effectively manage and mitigate the globally increasing (Hallegraeff 1993) HAB problem (Cloern 2001). Secondarily, we assessed the association between the bloom and fish kills that occurred a few days after the observed *K. veneficum* biomass maximum.

Methods and Materials

Study Site

The NRE is located along the central Atlantic seaboard of the USA (Fig. 1) and is a major tributary estuary of the Albemarle–Pamlico Sound estuarine system (Paerl et al. 1998; Peierls et al. 2003). The few narrow inlets in the outer banks of North Carolina restrict exchange with shelf waters, making the Albemarle–Pamlico Sound the largest lagoonal estuary in the USA. Astronomical tides in the NRE are negligible (Luettich et al. 2002). Riverine discharge and wind are the primary drivers of circulation, producing a

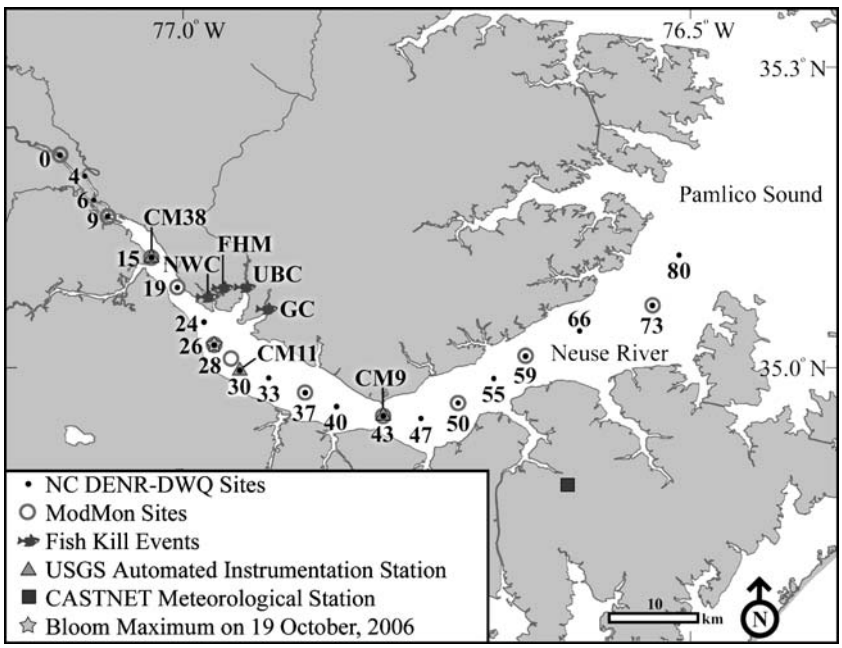

Fig. 1 Map of the Neuse River Estuary showing locations of sampling stations and documented fish kill events. Station identifiers are expressed as km downstream. USGS automated instrumentation stations are labeled by the channel marker (*CM*) to which they are fixed. *NWC* Northwest Creek, *FHM* Fairfield Harbor Marina, *BC* Broad Creek, and *GC* Goose Creek. Other acronyms are described in the "Methods and Materials"

partially mixed estuary where periods of strong salinity-based stratification are common (Luettich et al. 2000). Maximum depths along the axis of the estuary generally increase from approximately 4 m at the head of the estuary to near 7 m where the estuary empties into Pamlico Sound. Average depth is only 2.3 m because of extensive shelves and shoals that rim the estuary. The NRE has a history of algal bloom and hypoxia problems associated with anthropogenic nutrient loading (Paerl et al. 1998, 2004). As a result, it is currently under a legislated nitrogen load reduction plan (North Carolina Department of Environment and Natural Resources—Division of Water Quality, NCDENR-DWQ, 2001).

Sample Collection and Chemical Analyses

Shipboard data were obtained from 11 sites sampled as part of ModMon, a long-term monitoring program that collects bi-weekly water quality data (Luettich et al. 2000) and from 21 sites checked monthly by the North Carolina Department of Environment and Natural Resources, Division of Water Quality's (NCDENR–DWQ 2007). Station locations are expressed as distance downstream from the freshwater head of the estuary at Streets Ferry Bridge, New Bern, North Carolina (Fig. 1).

For chemical and plankton community analysis, samples were collected on 18 September, 3, 19, and 30 October 2006 by the ModMon monitoring program at all ModMon stations (Fig. 1). Samples were collected from the surface and from 0.5 m above the bottom using a Van Dorn sampler and dispensed in 2 l polyethylene bottles. Samples were transported in a dark cooler at ambient temperature to the laboratory within 4 h of collection. For nutrient analyses, 100 ml of each water sample was gently filtered through a pre-combusted Whatman 25-mm GFF filter, and the filtrate was frozen at −20°C within 6 h of collection. After nutrient filtration was completed, the filters were immediately frozen at −20°C for particulate C and N analyses. Subsequently, the frozen nutrient samples were quick thawed and $NO_2^- + NO_3^-$ (reported as NO_3^-), NH_4^+, PO_4^{-3}, and total dissolved nitrogen (TDN) immediately determined using a Lachat Quick-chem 8000 auto-analyzer (Lachat, Milwaukee, WI, USA; Lachat Quik-chem methods 31-107-04-3-B, 31-107-04-1-C, 31-107-06-1-B, and 31-115-01-3-C, respectively). During the analysis of each nutrient analyte, five replicates each of a high and low concentration quality control standard were interspersed throughout each run of environmental samples to determine measurement precision. The maximum observed coefficients of variation for $NO_2^- + NO_3^-$, NH_4^+, PO_4^{-3}, and TDN were 0.8%, 2.3%, 7.6%, and 11.4%, respectively. Dissolved inorganic nitrogen (DIN) was subtracted from TDN to obtain the dissolved organic nitrogen (DON) fraction. For particulate C and N analyses, filters were fumed at room temperature for 12 h with concentrated HCl to remove excess inorganic C and then analyzed on a Perkin–Elmer Series II 2400 CHNS/O analyzer.

Cell Counts

Subsamples of surface and bottom water from the ModMon stations were preserved in 1% Lugol's solution for phytoplankton and microzooplankton counts. Surface samples from ModMon stations 15–73, collected on 18 September, 3 October, 19 October, and 30 October, as well as the bottom water sample from the bloom maximum at station 26 on 19 October 2006, were counted using 15 ml settling chambers and a Leica DMIRB inverted microscope (Wetzlar, Germany) according to Utermöhl (1958). Cells within 40–100 random Whipple grids of the settling chamber base were identified and enumerated under phase contrast at a magnification of ×400. Ninety-five percent confidence intervals for each microscopic cell abundance estimate were calculated according to Clesceri et al. (1998).

For the region of the estuary where the highest *K. veneficum* biomass developed (ModMon stations 19, 26, 28, 37, and 43, hereafter called the bloom region), the average cell concentration of each phytoplankton species was calculated from surface water concentrations using a trapezoidal approximation procedure. Briefly, the mean cell concentration between each adjacent pair of stations in the bloom region was determined and multiplied by the distance between each respective station pair. These segmental estimates were then summed and divided by the total length of the bloom region to obtain a best estimate of the average cell concentration within the bloom region.

The net rate of change ($\mu_{apparent}$) in the abundance of *K. veneficum* and a number of other co-occurring plankton within the bloom region were then determined for the periods between 3–19 October and 19–30 October 2006. The equation used to calculate $\mu_{apparent}$ was $[\ln (N_f \times N_i^{-1})]\, t^{-1}$, where N_i and N_f are the initial and final average cell concentration for each sampling interval, calculated as described above, and t is the number of days between sample collection.

For microzooplankton, surface samples from the stations encompassing the bloom region were counted on 3 October, 19 October, and 30 October. A magnification of ×200 was used to count 200 random Whipple grids. Data are reported for four broad groups of microzooplankton: tintinnids, oligotrich ciliates >30 μm maximum dimension, *Oxyrrhis marina*, and other heterotrophic dinoflagellates >10 μm maximum dimension. These were chosen because they are of the size class capable of feeding on *K. veneficum* (Hansen et al. 1994). *O. marina* was separated from other heterotrophic dinoflagellates because it dominated heterotrophic dinofla-

gellate abundance during the study and is known to be an important grazer of *K. veneficum* (Johnson et al. 2003). Average concentrations of each microzooplankton group within the bloom region were calculated in the same manner as for the phytoplankton.

Surface water samples for phytoplankton enumeration were collected by NCDENR–DWQ at stations 15, 24, 30, 59, and 80 on 11 October 2006 and from the fish kill sites on 25 October, 30 October, and 1 November 2006 (Fig. 1). Cells were preserved in Lugol's amended with glycerin to preserve flagella (Vollenweider 1974) and counted according to NCDENR–DWQ protocols (http://h2o.enr.state.nc.us/esb/phytofolder/PhytoSOP_1_24_03.pdf) on a Leitz Diavert inverted microscope (Wetzlar, Germany) at ×500 magnification. All cells in random Whipple grid fields were counted until 100 cells of a single taxon were enumerated.

Physical Data

On 3, 19, and 26 October 2006, vertical profiles of temperature, salinity, dissolved oxygen (DO), in vivo fluorescence, and light at each ModMon station were made at 0.5-m intervals with a YSI 6600 multiprobe sonde coupled to a LiCor LI-1925A quantum sensor that measures photosynthetically active radiation (PAR) (Yellow Springs, Inc., Yellow Springs, OH, USA). Euphotic zone depth (1% surface irradiance) was calculated from the diffuse light attenuation coefficient derived from PAR profiles. In vivo fluorescence profiles were post-calibrated using the regression of in vivo fluorescence versus high-performance liquid chromatography (HPLC)-derived chlorophyll *a* (chl *a*) obtained from corresponding surface and bottom water samples. On 26 October, no water samples for HPLC chl *a* were collected, so the calibration curve from 19 October was used to calibrate fluorescence profiles. Contour plots of longitudinal and vertical salinity, DO, and chl *a* (from the calibrated fluorescence profiles) were produced using the 'contourf' function of Matlab version 7.0.0 R14 (http://www.mathwork.com, The Mathworks, Inc. Natick, MA, USA). All calculations and statistical analyses were also performed with Matlab version 7.0.0 R14.

Automated instrumentation operated by the US Geological Survey (USGS) at channel markers CM9 (34°56.917′ N, 76°48.583′ W), CM11 (34° 59.916′ N, 76°56.651′ W), and CM38 (35°06.567′ N, 77°01.967′ W; Fig. 1) provided measurements of surface (1 m) and bottom (3–3.5 m) temperature, salinity, and DO every 15 min using Hydrolab Surveyor IV water quality instruments (HACH Environmental, Loveland, Colorado). The station at CM11, closest to the bloom maximum, has been operational since 1989, allowing for the comparison of conditions during this study with historic norms (http://waterdata.usgs.gov/nc/nwis). Hourly wind and solar radiation data were obtained from the nearby US Environmental Protection Agency, Clean Air Status and Trends Network (CASTNET) site 142 (34°53.088′ N, 76° 37.218′ W; Fig. 1; http://www.epa.gov/castnet). Neuse River flow data were obtained from the USGS flow station at Kinston, NC, USA (http://waterdata.usgs.gov/nc/nwis), approximately 90 km upstream from the head of the NRE. Flow at this location averages two thirds of the total flow into the estuary (Luettich et al. 2000).

Photopigment, DNA, and Toxin Analyses

Photopigment analysis via HPLC was performed as described by Pinckney et al. (1996), except that the analyses were performed on a Shimadzu LC-20AB HPLC coupled to a Shimadzu SPD M20A in-line photodiode array spectrophotometer (Shimadzu-Benelux, Antwerpen, Belgium).

Total DNA for genetic confirmation and quantification of *K. veneficum* was extracted from Lugol's preserved samples using the Puregene kit from Gentra Systems (Minneapolis, Minnesota). One microliter was used as template in a real-time polymerase chain reaction (PCR) assay specific for the internal transcribed spacer locus (ITS) of the ribosomal DNA (rDNA) genome of *K. veneficum* (Bowers et al., unpublished data). Specificity of this assay has been confirmed against 45 *K. veneficum* cultures (all positive), as well as 26 closely related dinoflagellate species (all negative, including *K. armiger*, *K. conicum*, *K. australe*, and two *Karenia* species; Bowers H. A. et al., unpublished data). Each reaction contained 0.1 U *Taq* Pro (Denville Scientific, Metuchen, NJ, USA, PCR buffer, 3 mM $MgCl_2$, 0.2 μM forward and reverse primers, 0.3 mM each deoxynucleotide triphophosphate (Invitrogen, Alameda, CA, USA), 0.25 mg ml^{-1} bovine serum albumin (Idaho Technology, Idaho Falls, ID, USA), 0.3 μM Taqman probe, molecular grade water to 10 and 1 μl DNA template. Samples, controls, and a serial dilution of a plasmid containing the target insert (i.e., standard curve, prepared as described in Bowers et al. 2006) were run on the ABI 7500 (Applied Biosystems, Foster City, CA, USA). The following parameters were used: an initial denaturing step for 5 min at 95°C followed by 50 cycles of 15 s at 95°C, and 30 s at 60°C.

Samples for karlotoxin (KmTx 2) analysis taken at the peak of the bloom on 19 October were collected on polytetrafluoroethylene filters that quantitatively retained particulate and dissolved toxin (Bachvaroff et al. 2007). Concentrations were measured by liquid chromatography–mass spectrometry (LC–MS) using a C8 HPLC column (LiChrosphere, 125× 4 mm 5-μm bead size RP-8, Waters Corporation) and an Agilent G1956A VL mass spectrometer. Karlotoxin peaks previously shown to have hemolytic activity were quantified based on calibration curves derived from pure KmTx 2 (Bachvaroff et al. 2007). Hemolytic assays of 15 s HPLC fractions from the bloom samples were performed using

striped bass (*Morone saxatilis*) erythrocytes to confirm hemolytic activity of the KmTx 2 fraction. Saponin (10 μg; Sigma Chemical Co.) was used as a positive hemolysin control according to Eschbach et al. (2001).

Results

Bloom Characteristics

On 19 October 2006 at station 26, a dense dinoflagellate bloom producing obvious water discoloration was discovered. *K. veneficum* cell abundance exceeded 200,000 cells per milliliter (Table 1) and numerically dominated the phytoplankton assemblage (Table 2). The photopigment signature from the bloom samples was consistent with that obtained from cultured *K. veneficum* and included very high chl *a*, fucoxanthin, 19′ hexanoyloxyfucoxanthin (19′-hex), 19′ butanoyloxyfucoxanthin (19′-but), chlorophyll *c3*, diadinoxanthin, chl *c1–c2*, and gyroxanthin diester (Table 1; Kempton et al. 2002). In addition to *K. veneficum*, the bloom also contained high concentrations of other potentially bloom-forming dinoflagellates (Campbell 1973) that contained peridinin, as well as fucoxanthin-containing *Leptocylindrus minimum*, a small-chain forming diatom, alloxanthin-containing cryptophytes, and chlorophyll *b*-containing euglenoids, and chlorophytes (Tables 1 and 2). *K. veneficum* was likely the sole contributor of 19′-hex, gyroxanthin, and 19′-but, which are characteristic of this species, but found in few other dinoflagellates (Kempton et al. 2002). The 19′-hex concentration observed at the bloom maximum was 93.9 μg l^{-1} (Table 1). The next highest value in the ModMon pigment database, which included 5,923 measurements of 19′-hex in the NRE from 4 January 1994 to 30 October 2006, was 1.93 μg l^{-1}.

Two putative karlotoxin peaks were detected from the bloom samples by the LC–MS analysis, one eluting at 9.1 min and one at 14.8 min (Fig. 2a). The mass spectra of the bloom samples contained the major ion (1,367.8 amu) of purified KmTx 2 (Bachvaroff et al. 2007) but also contained a congener that is 16 amu lower (data not shown). The UV absorption spectrum of the toxin isolated from the bloom was identical to purified KmTx 2 (data not shown) with a maximum absorbance of 235 nm (Bachvaroff et al. 2007). The mass spectrum of the 9.1-min peak was consistent with sulfated congeners of the ions present in the 14.8-min peak (data not shown). Toxin isolated from the 14.8-min peak coeluted with the KmTx 2 standard (Fig. 2b), and the hemolytic activity of the toxin in this fraction was confirmed by a near 100% erythrocyte hemolysis rate as compared to the Saponin control (Fig. 2b).

K. veneficum cell abundance and toxin concentration were highly localized at station 26 (Fig. 3), and the linear relationship between toxin and cell abundance was highly significant (R^2=0.99, $P<1\times10^{-7}$). Cell abundance and ITS rDNA copy number determined using quantitative PCR (qPCR) also tracked each other closely throughout the study (Fig. 3; R^2=0.9995, Table 3). This highly significant correlation between the qPCR results and microscopic counts indicates both independent methods accurately quantified *K. veneficum* abundance and that there were approximately 67 detectable ITS sequences per *K. veneficum* cell in situ.

Table 1 Summary of surface and bottom *K. veneficum* abundance, particulate organic carbon, particulate nitrogen, and photopigment data from the bloom maximum at station 26 on 19 October 2006

Property	Concentration	
	0 m	3 m
Karlodinium veneficum, cells per milliliter (95% confidence interval)	219,481 (213,621–225,340)	626 (279–973)
Mean particulate organic carbon, μM (standard deviation)	1,138 (3.1)	202 (0.5)
Mean particulate nitrogen, μM (standard deviation)	185 (10.8)	21.7 (0.5)
Photopigments, μg l^{-1}		
chlorophyll *a*	257.3	21.8
Fucoxanthin	222.2	6.6
19′ Hexanoyloxyfucoxanthin	93.9	0.95
Chlorophyll *c3*	81.5[a]	1.8[a]
Diadinoxanthin	59.0	1.4
19′ Butanoyloxyfucoxanthin	33.6	0.35
Chlorophyll *c1–c2*	32.0	1.1
Gyroxanthin diester	32.1	0.32
Peridinin	12.4	1.1
Chlorophyll *b*	9.0	0.17
Alloxanthin	2.3	0.09
Zeaxanthin	0	0.29
Chlorophyllide *a*	0	0
9′ *cis*-Neoxanthin	0	0
Violaxanthin	0	0
Antheraxanthin	0	0
Monadoxanthin	0	0
Lutein	0	0
β-Carotene	0	0
Myxoxanthophyll	0	0

Chlorophyll *c3* eluted at the appropriate time but the absorbance spectrum was shifted toward the red by ±1 nm over the time course of the peak indicating incomplete separation from another pigment/pigments.

Bloom Chronology

River flow before Tropical Storm Ernesto (1 September 2006) was below the 50-year median value (48 m^3 s^{-1}) but increased rapidly after the storm to more than four times the median flow (Fig. 4). The main body of the floodwater

Table 2 Average abundance and apparent growth rates of dominant phytoplankton and microzooplankton species within the bloom region (ModMon stations 19, 26, 28, 37, and 43) during the bloom growth (3–19 October) and collapse (19–30 October) phases

Cell type	Abundance (cells per milliliter)			$\mu_{apparent}$ (per day)	
	October			October	
	3	19	30	3–19	19–30
Dinoflagellates					
Karlodinium veneficum	801	43,575	150	0.25	−0.52
Peridinium aciculiferum	54	453	1	0.13	−0.60
Heterocapsa rotundata	331	435	7	0.02	−0.38
Scrippsiella trochoidea	70	275	2	0.09	−0.43
Pheopolykrikos hartmanii	17	105	1	0.11	−0.47
Cryptophytes					
Cf. *Hemiselmis virescens*	565	1,383	0	0.06	NA
Cf. *Chroomonas minuta*	1,037	1,597	229	0.07	−0.10
Cryptomonas sp.?	601	37	245	−0.17	0.17
Teleaulax amphioxeia	1,050	2,933	1,025	0.03	−0.18
Diatoms					
Cylindrotheca closterium	99	1,365	197	0.16	−0.18
15 μm length pennate	0	6,323	2,032	NA	−0.10
Leptocylindrus minimum	65	19,985	25,517	0.36	0.02
<8 μm diameter centric	880	624	404	−0.02	−0.04
Skeletonema costatum	170	425	1,570	0.06	0.12
Aulacoseira sp.	540	77	746	−0.12	0.21
Chlorophytes					
Pyramimonas sp.	1,028	1,283	161	0.01	−0.19
Chlamydomonas sp.	605	1,403	384	0.05	−0.12
Euglenophytes					
Eutreptia lanowii	39	494	38	0.16	−0.23
Cyanobacteria					
Planktolyngbya sp.[a]	302	5,394	1,483	0.18	−0.12
Other small flagellates	4,986	9,687	2,548	0.04	−0.12
Microzooplankton					
>30 μm oligotrich ciliates	2	14	14	0.12	0
Tintinnid ciliates	3	26	13	0.13	−0.06
Oxyrrhis marina	33	118	119	0.08	0.00
Other heterotrophic dinoflagellates >10 μm	25	33	53	0.02	0.04

NA $\mu_{apparent}$ could not be calculated because either the initial or final abundance was zero.
[a] Abundance of *Planktolyngbya* sp. is in filaments per milliliter.

pulse reached the estuary ~10 days after the storm and freshened the estuary from surface to bottom (Fig. 4). As flow rates declined, the resumption of estuarine circulation was apparent as increases in bottom salinity. The progression of the salt wedge upstream as flow declined is clearly evident from the three real-time data sets (Fig. 4). The salt wedge passed CM9 on 13 September 2006 (Fig. 4), followed by CM11 on 14 September (Fig. 4), and finally, reached CM38 on 16 September (Fig. 4). Based on the time and distance traveled, upstream bottom water velocities were 13 cm s^{-1} from 13–14 September (CM9 to CM11), 6 cm s^{-1} from 14–16 September (CM11 to CM38), and 11 cm s^{-1} for the 13–16 September upstream advance from CM9 to CM38. At the end of the high-flow period on 18 September, *K. veneficum* was observed only at the most downstream stations, with a maximum abundance of ~100 cells per milliliter (Fig. 3).

Strong estuarine circulation resumed as riverine discharge declined and, in combination with weak winds, led to an unusually protracted period of stratification that lasted from 14 September to 6 October 2006 (Fig. 4). At the CM11 station, the minimum difference in salinity between the top and bottom over the 22-day period was 4.6 ppt. Historical records of surface and bottom salinities from 13 May 1989 to 6 October 2006 at CM 11 (6,355 observations) showed that similar 22-day periods with a continuous minimum vertical salinity difference of 4.6 occurred only 0.7% of the time.

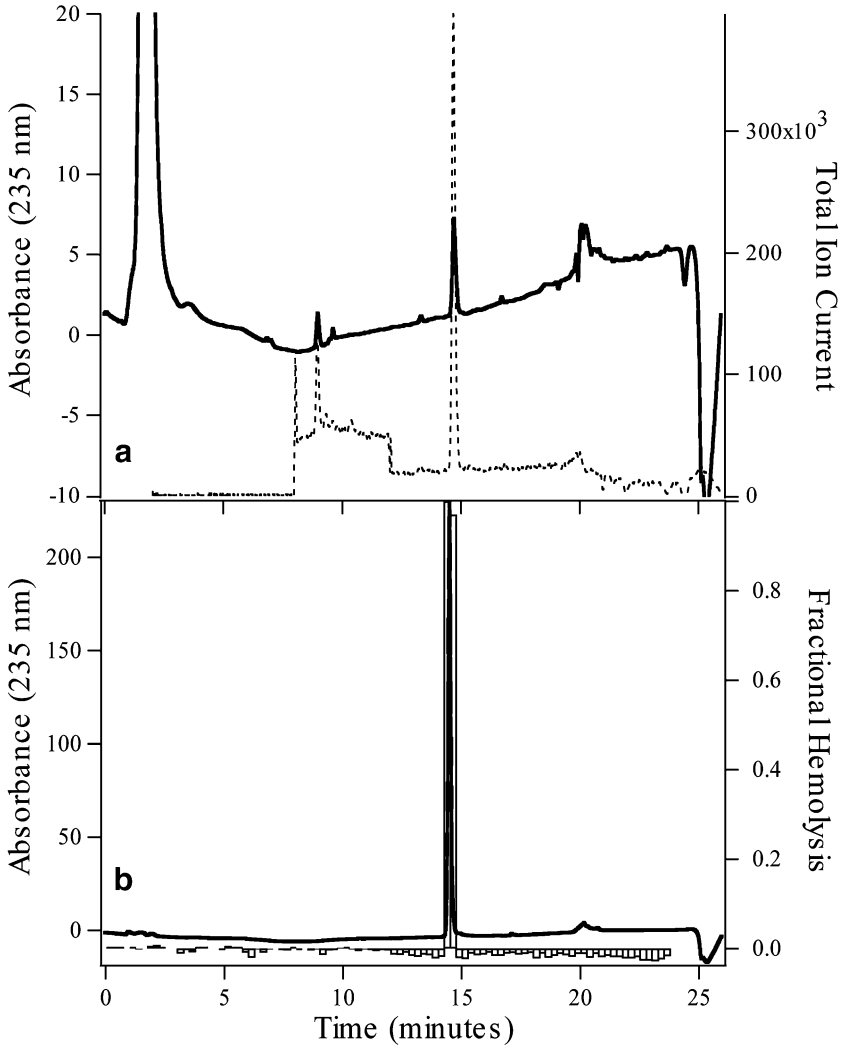

Fig. 2 Toxin analysis from the bloom sample collected on 19 October 2006 at station 26. (**a**) HPLC elution profile of the methanol extract of the bloom sample monitored by absorbance at 235 nm (*solid line*) and total ion current (*dashed line*) from the mass spectrometer at ions ranging from 500 to 1,500 amu. **b** Hemolytic activity of the HPLC fractions collected every 15 s from the bloom sample (*bars*) and the HPLC elution profile of purified KmTx 2 at 235 nm (*solid line*)

On 3 October 2006, surface temperature was ~23°C (Fig. 5), and the estuary was strongly stratified from station 9 to the mouth of the estuary (Fig. 6). Surface salinity increased in a nearly linear fashion from 0 to 13 ppt from the head to mouth of the estuary (Fig. 6). Irradiance was high with a mid-day maximum of 750 W m^{-2} (Fig. 5). Significant correlations between extracted chl *a* and in vivo fluorescence were obtained, which allowed postcalibration of in vivo fluorescence (Table 3) to estimate vertical and horizontal phytoplankton biomass distributions. At stations 26, 43, and 59, three subsurface peaks in chl *a* greater than 20 μg l^{-1} were located at approximately 0.75- to 1.0-m depths (Fig. 6). Euphotic zone depths increased from ~2 m at the head to ~4 m at the mouth of the estuary (Fig. 6). The hypolimnion was severely hypoxic, whereas the epilimnion was DO supersaturated from station 19 to the mouth of the estuary (Fig. 6). Surface and bottom water NO_3^- decreased from 50 μM at the head of the estuary to below detection (0.04 μM detection level) at stations 43 and 19, respectively (Fig. 6). Both surface and bottom DON concentrations were relatively constant at ~30 μM (Fig. 6). Bottom water concentrations of NH_4^+ and PO_4^{-3} were unusually high (Fig. 6). Peak values, 38 μM NH_4^+ and 6.3 μM PO_4^{-3} were in the 99th percentile of 3,294 observations of bottom water NH_4^+ and PO_4^{-3} from the NRE over the last 21 years. *K. veneficum* cells were present from stations 26 to 73 with a population maximum of ~4,000 cells per milliliter at station 43 (Fig. 3).

A strongly stratified condition was maintained through 6 October (Fig. 5). On 7 October, a wind event (Fig. 5) thoroughly mixed the water column. Normoxic hypolimnetic conditions were restored (Fig. 5), and a large pulse of NH_4^+ and PO_4^{-3} was mixed throughout the water column.

On 11 October, *K. veneficum* concentrations were higher than on 3 October, and the population maximum of ~15,000 cells per milliliter was located further upstream at NC DENR–DWQ station 24 (Fig. 3).

From 11–17 October, conditions were sunny (Fig. 5), winds were light (<3 m s^{-1}; Fig. 5), and the estuary was weakly stratified (Fig. 5). On 17 October, passage of a

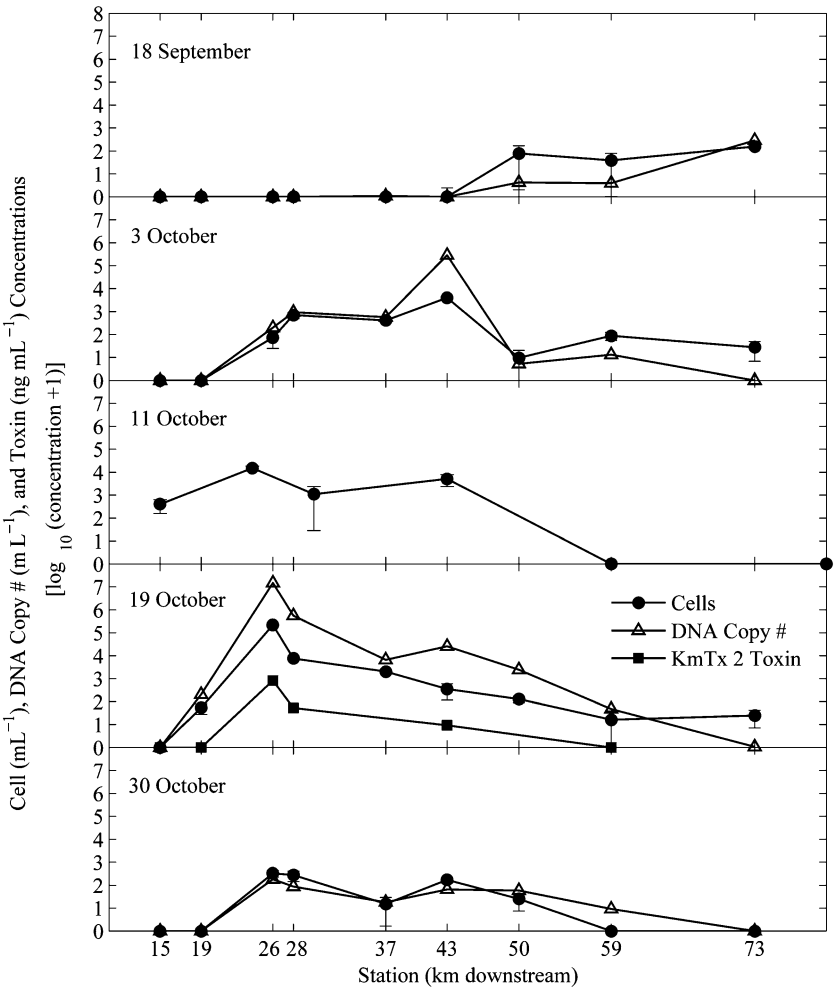

Fig. 3 Downstream distribution of surface water *K. veneficum* cell abundance and DNA copy number on five sampling dates spanning the bloom period. *Error bars* for cell abundance data are the 95% confidence interval for the microscopic abundance measurement. KmTx 2 toxin concentration is shown for 19 October 2006

warm front warmed the water by ~3°C (Fig. 5) and was accompanied by heavy cloud cover that reduced irradiance to mid-day maxima of only ~300 W m^{-2} from 17 October through 19 October (Fig. 5). During this period, declining bottom DO concentrations indicated low vertical mixing (Figs. 5 and 7).

From 3–19 October, nearly all phytoplankton species within the bloom region experienced positive growth (Table 2). The *K. veneficum* population within the bloom region grew at 0.25 per day (Table 2), an apparent growth rate greater than all other co-occurring phytoplankton species with the exception of *L. minimum* (Table 2). Two species of 4- to 10-µm cryptophytes, cf. *Chroomonas minuta* and cf *Hemiselmis virescens* (Campbell 1973), were abundant throughout the study. Small cryptophytes such as these are preferred prey items for *K. veneficum* (Li et al. 2000). The

Table 3 Regression equations and statistical results of HPLC chlorophyll *a* (chl *a*) on in vivo fluorescence and toxin concentration and DNA copy # on *K. veneficum* cell abundance

Regression variables	N	Slope (95% C. I.)	Intercept (95% C. I.)	R^2	P
Chlorophyll *a* on in vivo fluorescence (3 October)	19	0.78 (±0.28)	−0.48 (±3.27)	0.66	<0.005
Chlorophyll *a* on in vivo fluorescence (19 October)	22	0.72 (±0.04)	3.29 (±2.60)	0.99	$<1\times10^{-20}$
Toxin KmTx 2 on *K. veneficum* abundance (19 October)	6	$3.70\text{x}10^{-3}$ ($\pm0.15\text{x}10^{-3}$)	4.02 (±13.6)	0.99	$<1\times10^{-7}$
DNA copy no. on *K. veneficum* abundance (18 Sep., 3, 19, 30 Oct.)	36	67.0 (±0.03)	−8,466 (±11,730)	0.99	$<1\times10^{-4}$

Chl *a* (µg l^{-1})=in vivo fluorescence (units l^{-1}) × slope (µg per unit) + intercept (µg l^{-1}); KmTx 2 (ng ml^{-1})=*K. veneficum* (cells ml^{-1}) × slope (ng cell^{-1}) + intercept (ng ml^{-1}); DNA copy no. (number per milliliter)−*K. veneficum* (cells per milliliter) × slope (number per cell) + intercept (number per milliliter)

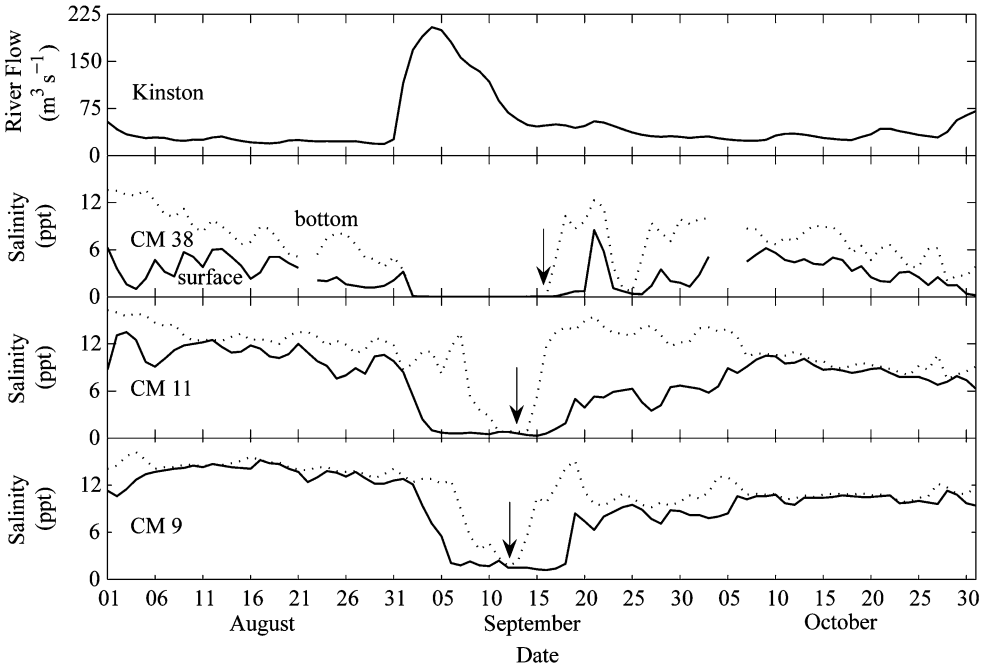

Fig. 4 Time series of riverine discharge and salinity. Neuse River discharge at Kinston, NC (*top panel*), and surface (*solid line*) and bottom (*dotted line*) salinity from three USGS automated instrumentation at channel markers CM 38, CM 11, and CM 9 (*lower panels*). *Arrows* indicate the timing of the intrusion of the salt water layer after the flushing event from Tropical Storm Ernesto

sum of these two small cryptophytes closely tracked the *K. veneficum* population and reached a maximum abundance within the bloom region of ~3,000 cells per milliliter on 19 October 2006 (Table 2). Large (>30 μm) oligotrich ciliates, tintinnids, and *O. marina* abundances increased as the bloom developed, reaching 14, 26, and 118 cells per milliliter, respectively, on 19 October (Table 2).

At the *K. veneficum* bloom maximum (station 26, 19 October), approximately 80% of water column chl *a* was within the upper 1 m (Fig. 7). Horizontally, the maximum of *K. veneficum* and chl *a* was located along a frontal region, marked by a steep surface salinity gradient that separated the strongly stratified region upstream from the less-stratified downstream region (Fig. 7). The other

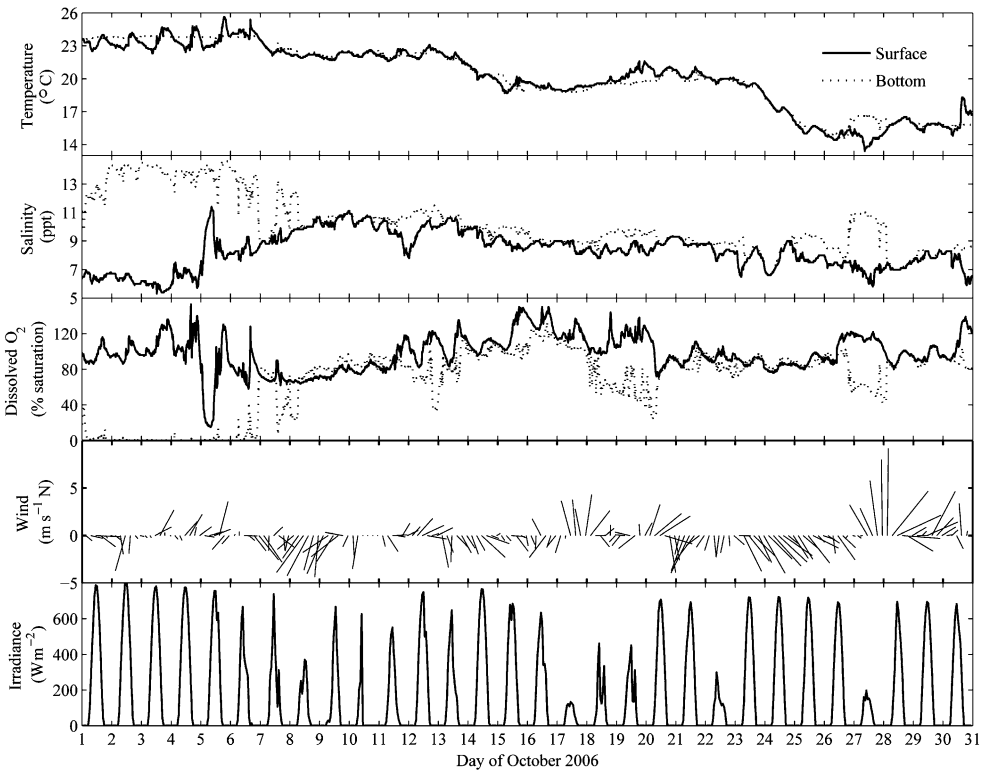

Fig. 5 Time series of environmental data from channel marker CM 11 for the bloom period, October 2006. Surface (*solid line*) and bottom (*dashed line*) temperature, salinity, and dissolved oxygen measured every 15 min. Four-hour block-average vectoral wind speed. Hourly block-average ground level solar irradiance

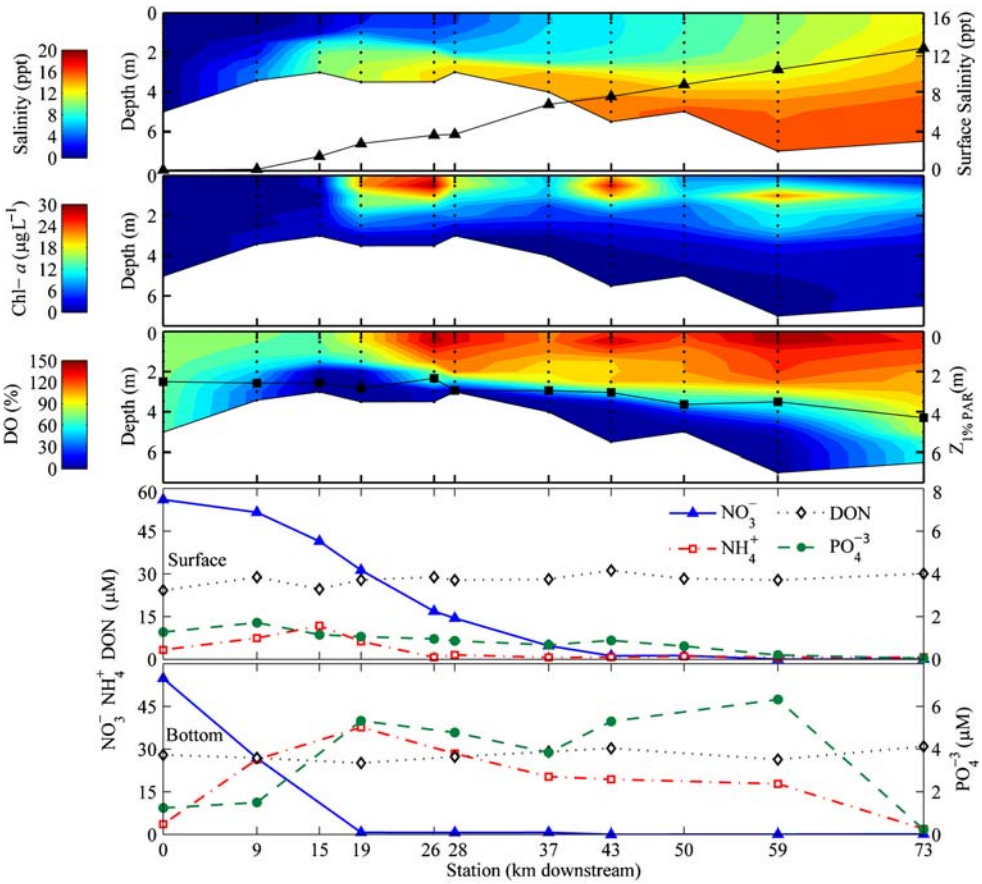

Fig. 6 Estuarine conditions in the downstream and vertical dimensions on 3 October 2006. Contour plots of salinity, dissolved oxygen, and chlorophyll *a*. Contour magnitudes are given by the *scale bar to the left of the figure*. Sampling locations are indicated by *dots*. Surface salinity is overlain on the salinity contour plot (*solid line* and *triangles*). The depth of 1% incident PAR is overlain on the dissolved oxygen plot (*solid line* and *squares*). Downstream distributions of surface and bottom water nutrient concentrations. DON (black *dotted line*, *open diamonds*), NO_3^- (blue *solid line*, *solid triangles*), NH_4^+ (red *dash–dot line*, *open squares*), PO_4^{-3} (right *y*-axis, green *dashed line*, *solid circles*)

dinoflagellates common in the bloom region showed a similar accumulation of biomass at station 26 (Fig. 8), whereas the most abundant diatoms displayed monotonic increases or decreases through the frontal region (Fig. 8). At station 26, the *K. veneficum* population increased from 73 cells per milliliter on 3 October to 219,000 cells per milliliter on 19 October (Fig. 3). This increase represents an apparent growth rate of 0.5 per day, which was double the rate of *K. veneficum* when calculated over the bloom region as a whole (Table 2).

On 19 October, DIN was reduced to ~1 μM within and downstream of the bloom maximum (Fig. 7). The downstream distribution of surface and bottom water DON was relatively constant at approximately 25 μM, except in the bloom maximum located at the surface of station 26. Here, DON was more than twofold higher than at any other station measured on either 19 October or on 3 October (Figs. 6 and 7). Like DON, PO_4^{-3} was much higher within the bloom than in the surrounding stations (Fig. 7). Based on the particulate nitrogen measurement from the bloom (185 μM, Table 1) and assuming a cellular N/P molar ratio of 9 (Nielsen 1996), the excess DON and PO_4^{-3} within the peak of the bloom, relative to adjacent stations, constituted only 12–13% of the total N and P pools found in the phytoplankton.

On the morning of 20 October 2006, strong (~6 m s^{-1}) southwest winds mixed the water column (Fig. 5). As the day progressed, wind direction rotated clockwise nearly 180°, resulting in an ~5 m s^{-1} northeast wind by the following morning (Fig. 5). Starting on 23 October, a cold front accompanied by moderate (~5 m s^{-1}) northwest winds (Fig. 5) cooled the estuary by ~5°C over a 3-day period (Fig. 5).

On 26 October, maximum chl *a* values were less than 20 μg l^{-1}, showing that the bloom had dissipated by this time (Fig. 9). Salinity between 19 and 26 October showed no evidence of a major washout event (Fig. 5). Irradiance was high (>700 W m^{-2}), and the bulk of chlorophyll within the bloom region was distributed as a subsurface maximum at ~2 m, extending from station 28 downstream to at least station 43 (Fig. 9). By 30 October 2006, maximal concentrations of *K. veneficum* were ~300 cells per milliliter (Fig. 3). The apparent growth rate from 19–30 October of the population within the bloom region was −0.52 per day (Table 2). Other common photosynthetic dinoflagellates experienced similarly large population losses (−0.38 to −0.60 per day; Table 2). Phytoplankton other than dinoflagellates experienced only slight declines or moderate increases over the same time period (Table 2). Large (>30 μm) oligotrich ciliates and the heterotrophic

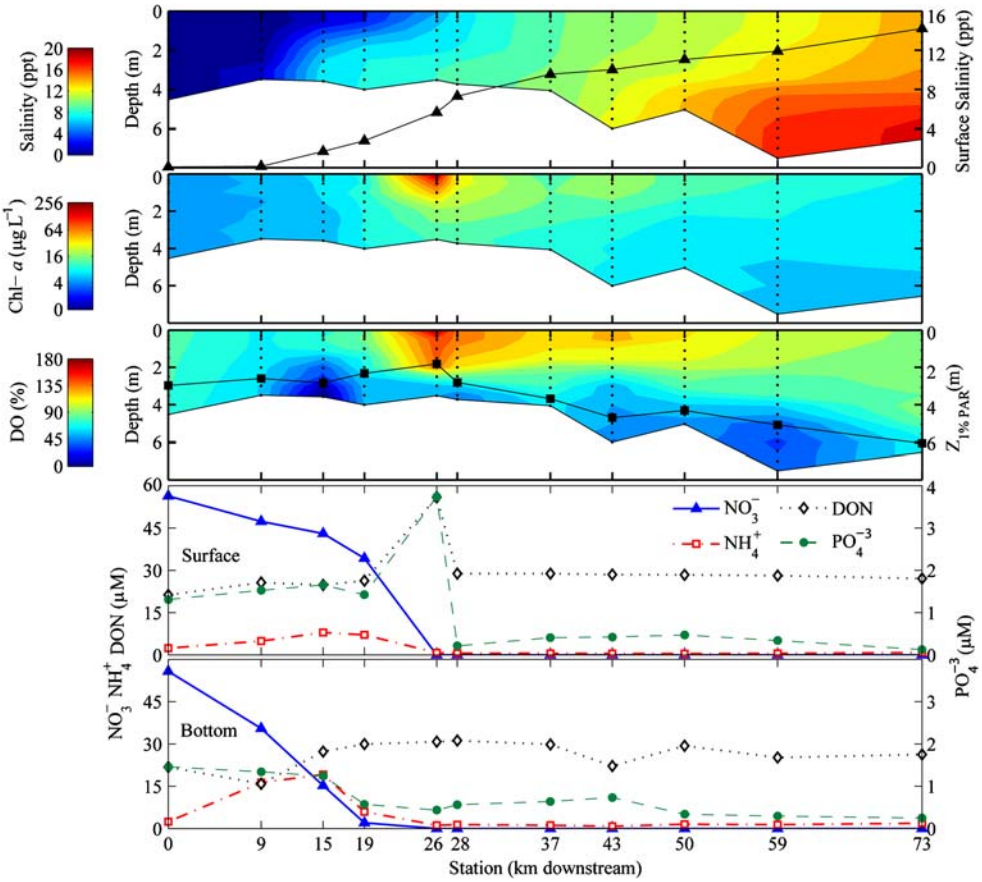

Fig. 7 Estuarine conditions in the downstream and vertical dimensions on 19 October 2006. Contour plots of salinity, dissolved oxygen, and chlorophyll *a*. Contour magnitudes are given by the *scale bar to the left of the figure*. Note $\log_2$ scale for chlorophyll *a*. Sampling locations are indicated by *dots*. Surface salinity is overlain on the salinity contour plot. The depth of 1% incident PAR is overlain on the dissolved oxygen plot. Downstream distributions of surface and bottom water nutrient concentrations. DON (*black dotted line* and *open diamonds*), NO_3^- (*blue solid line* and *solid triangles*), NH_4^+ (*red dash–dot line* and *open squares*), PO_4^{3+} (right *y*-axis, *green dashed line* and *solid circles*)

dinoflagellate *O. marina* abundances remained constant over this period. The other >10-µm heterotrophic dinoflagellates besides *O. marina* nearly doubled, whereas tintinnid abundance decreased by half (Table 2).

Fish Kills

Four days after the observed bloom maximum at station 26 on 19 October, a resident living on Upper Broad Creek (Fig. 1) noticed fish gulping air at the surface. The next day, 24 October, the resident reported that the fish were dead and another fish kill report was made for Northwest Creek (Fig. 1, Table 4; NCDENR Fish Kill Database 2006). *K. veneficum* concentrations of ~2,500 cells per milliliter were observed in Northwest Creek on 25 October. Two more fish kills were reported on 29 October and 1 November, but the decayed condition of the fish led to the conclusion that they occurred at the same time as the prior two fish kills. *K. veneficum* concentrations at the latter two fish kill sites were ~300 cells per milliliter. A variety of common estuarine and brackish-water-tolerant freshwater species were killed (Table 4). Salinities in the fish kill waters were approximately the same as at the bloom maximum. There were no other apparent causes for fish kills such as temperature stress, hypoxia, chemical spills, or bycatch release by fishermen.

Discussion

The magnitude of the *K. veneficum* bloom observed in this study is unprecedented in North Carolina estuaries, exceeding previously reported maximum cell concentrations by nearly an order of magnitude (Fensin 2004). Growth of the bloom was largely attributable to abnormally high nutrient availability, a prolonged period of water column stability, and reduced dispersal. Hydrodynamic conditions along a salinity front further concentrated the toxin containing *K. veneficum* cells to high densities (>200,000 cells per milliliter and >800 ng KmTx 2 ml^{-1}). The toxin content of these cells, if released, was more than sufficient to cause fish mortality (Kempton et al. 2002; Deeds et al. 2006).

Bloom Initiation

Meteorological forcing events that alter nutrient inputs, temperatures, stratification, or flow regimes in significant ways often select for bloom organisms that are not normally dominant in an ecosystem. One such example was a "surprise" dinoflagellate bloom in San Francisco Bay, which is usually dominated by diatoms. This bloom resulted from a period of high air temperatures, low wind stress, and thermal stratification that allowed dinoflagellates to grow and accumulate in an abnormally shallow upper

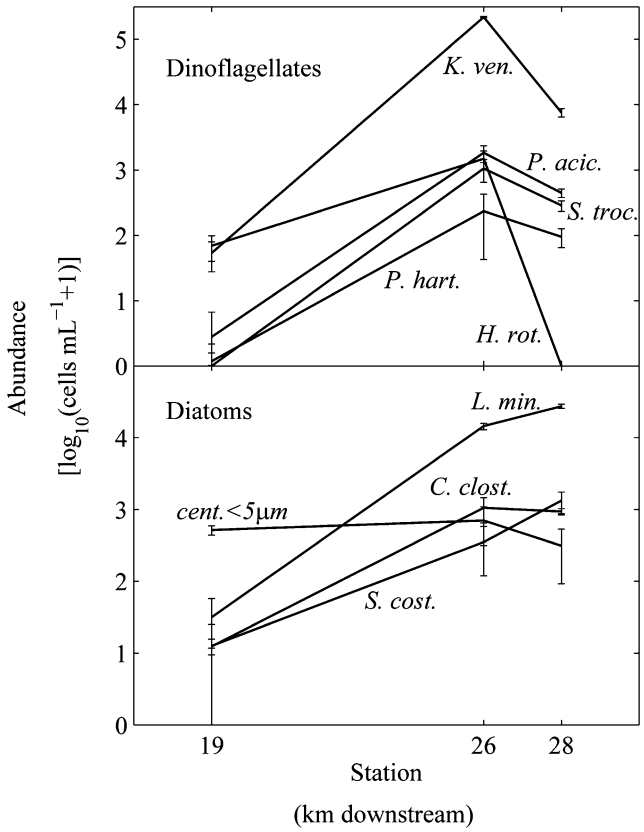

Fig. 8 Surface water abundance of the numerically dominant dinoflagellates and diatoms at the three stations (19, 26, and 28) encompassing the frontal region on 19 October 2006. *K. ven.*, *Karlodinium veneficum*; *S. troc.*, *Scrippsiella trochoidea*; *P. hart.*, *Pheopolykrikos hartmanii*; *P. acic*, *Peridinium aciculiferum*; *H. rot*, *Heterocapsa rotundata*; *L. min.*, *Leptocylindrus minimum.*; *S. cost.*, *Skeletonema costatum*; *C. clost.*, *Cylindrotheca closterium*; *cent <5 μm*, non-chain-forming centric diatoms <5 μm in diameter. *Error bars* are the 95% confidence intervals for microscopic abundance measurements

mixed layer (Cloern et al. 2005). In the Chesapeake Bay, an unusual fall diatom bloom was initiated when wind mixing from Hurricane Isabel injected bottom water nutrients into the surface waters (Miller et al. 2006). For the *K. veneficum* bloom described in this study, the unusual meteorological event was flooding from Tropical Storm Ernesto, which was followed by a 3-wk period of uninterrupted water column stratification.

In addition to a precipitating forcing event, which species subsequently dominates, the assemblage also depends on the availability of a seed population (Steidinger 1983). In the NRE, *K. veneficum* is nearly always found at background concentrations (Fensin 2004; Litaker R. W., unpublished data). However, the cell count and qPCR data (Fig. 3) clearly indicate that discharge from Tropical Storm Ernesto initially flushed the background population out of the bloom region. The most likely source of cells was the small population near the mouth of the estuary, which was subsequently transported into the bloom region via subsurface transport. Support for this transport comes from the fact that following the washout from Tropical Storm Ernesto, as flow rates declined, the salt wedge moved upstream at a rate of 6–13 cm s^{-1}. These values are in the range for acoustically measured bottom-water velocities in the NRE (Luettich et al. 2000) and were adequate to move cells 30 km upstream from 18 September to 3 October 2006. A similar subsurface transport mechanism inoculates the upper Chesapeake Bay with bloom-forming dinoflagellates annually (Tyler and Seliger 1978; Li et al. 2000).

Coincident with this subsurface transport, the water column became strongly stratified, allowing the accumulation of high concentrations of sediment-derived NH_4^+ and PO_4^{-3} in the hypolimnion (Fig. 6). A significant portion of these regenerated nutrients were mixed into the surface waters during the wind event of 7 October 2006, supplying nutrients without the significant dilution that occurred immediately after Tropical Storm Ernesto (Fig. 6).

Growth Phase of the Bloom

After the mixing event, the apparent growth rate of the *K. veneficum* population within the bloom region (0.25 per day, Table 2) was close to the maximum autotrophic intrinsic growth rate of strains isolated from southeast US estuaries (0.32 to 0.38 per day; Li et al. 1999; Adolf et al. 2003, 2006a). Water temperature (~20°C) and the prevailing mesohaline conditions were conducive for *K. veneficum* growth (Nielsen 1996; Li et al. 2000; Fensin 2004; Goshorn et al. 2004). Prior studies have shown that algal blooms are common in the region of the estuary where this bloom developed (Valdes-Weaver et al. 2006; Waggener 2006). One explanation is that the estuary widens in this region, increasing the residence time with respect to riverine discharge (Luettich et al. 2000). Reduced advective losses and continuous nutrient supply from both riverine discharge and the underlying sediments lead to biomass accumulation as was observed during this bloom (Pinckney et al. 1997; Waggener 2006). The general favorability for phytoplankton growth in the bloom region was demonstrated in this

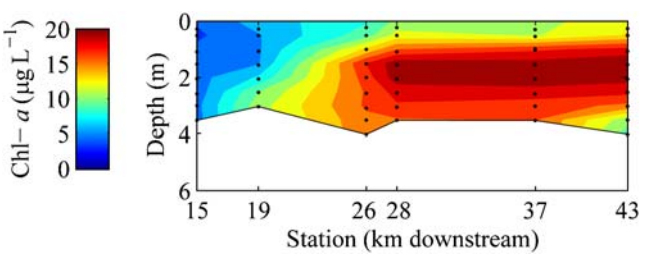

Fig. 9 Downstream and vertical distribution of chlorophyll *a* within the bloom region on 26 October 2006. Contour magnitudes are given by the *scale bar to the left of the figure*. Sampling locations are indicated by *dots*

Table 4 Summary of fish kill investigations after the observed *K. veneficum* bloom

Location and date of fish kill investigation	Fish affected	Environmental conditions	*Karlodinium veneficum* abundance in cells per milliliter (95% CI)	Notes
Upper Broad Creek 24 October 2006 16:00 35°04.7466′ N 76°56.2314′ W	Total ~502, speckled trout (30), southern flounder (15), Atlantic menhaden (15), spot (406), large mouth bass, pumpkin seed	Temperature=17.9°C, salinity=7.6 ppt, DO=7.9 mg l^{-1}, pH=7.4	Not assessed	Reported on 24 October 2006. Fish were gulping from the surface on 23 October 2006
Northwest Creek 25 October 2006 09:42 35°04.2480′ N, 76°58.4718′ W	Total ~726, spot (327), gizzard shad (80), southern flounder (58), Atlantic menhaden (36), large mouth bass, pumpkin seed	Temperature=14.8°C, salinity=7.3 ppt, DO=9.6 mg l^{-1}, pH=7.4	2,541 (620–4,462)	Reported on 24 October 2006. Fish were dying at time of investigation
Goose Creek 30 October 2006 12:00 35°03.5202′ N, 76°54.9492′ W	Total not assessed, southern flounder (2), speckled trout (13), sunfish (13)	Temperature=17.0°C, salinity=6.0 ppt, DO=13.0 mg l^{-1}, pH=9	363 (1–1,089)	Reported on 29 October 2006. Fish were decayed. Kill was several days old
Fairfield Harbor Marina 01 November 2006 10:00 35°04.7316′ N, 76°57.4674′ W	Total ~4,050, bream (825), gizzard shad (276), crappie (103), large mouth bass (123), yellow perch, speckled trout, spot, striped bass, striped mullet, bay anchovy	Temperature=20.5°C, salinity=5.7 ppt, DO=7.0 mg l^{-1}, pH=7.0	363 (1–1,089)	Reported on 01 November 2006. Fish were decayed. Kill was several days old

study by increases in nearly all phytoplankton species as the *K. veneficum* population proliferated from 3 to 19 October (Table 2).

Under poorly mixed conditions, dinoflagellates can outcompete other phytoplankton by vertically migrating to access light and nutrient resources (Smayda 1997). Salinity data indicated that moderate stratification within the bloom region was common throughout the growth phase of the bloom, even after the mixing event of 7 October (Fig. 5). The observations of subsurface chl *a* maxima on 3 October and 26 October (sunny days) and surface accumulation on 19 October (overcast day) also show that vertical mixing rates within the bloom region were often low compared to phytoplankton swimming speeds and are consistent with vertical migrations to achieve light levels optimum for photosynthesis (Ault 2000).

The interaction between vertical migrations and the prevailing frontal circulation pattern most likely produced the peak in biomass discovered at station 26 on 19 October. Frontal circulation patterns, particularly a two-layer flow and convergent downwelling, are known to retain and even concentrate vertically migrating phytoplankton (Chang and Carpenter 1985; Janowitz and Kamykowski 2006). The importance of the interaction between vertical migration and frontal circulation was clear from differences in the relative abundance of diatoms and dinoflagellates at the three sites encompassing the frontal region (Fig. 8). Nonmotile diatoms did not accumulate in the front but rather showed monotonic increases or decreases across the frontal boundary. In contrast, the vertically migrating dinoflagellates were horizontally concentrated at the frontal boundary (Fig. 8).

At the time of sampling (midday), the bloom population was also skewed toward the surface (Fig. 7). This was probably a positive phototaxic response to alleviate light limitation caused by the low incident irradiance from 17–19 October (Fig. 5). Thus, the surface bloom maximum on 19 October was caused primarily by the hydrodynamic accumulation at the frontal region and secondarily to positive phototaxis. The dominance of hydrodynamics in concentrating the cells is supported by the fact that dinoflagellates did not accumulate to nearly the same degree at adjacent stations.

While our data show that conditions were conducive for phytoplankton growth in general and, likely, dinoflagellates in particular, the question arises as to why *K. veneficum* came to dominate the phytoplankton assemblage. We speculate that one reason is that *K. veneficum*'s toxin, KmTx 2, acted as a grazing deterrent and gave *K. veneficum* an advantage over other phytoplankton. Microzooplankton and ciliates, in particular, have growth rates comparable to their phytoplankton prey and can exert high-grazing pressures on algal blooms (Watras et al. 1985;

Nakamura et al. 1996). Microzooplankton abundance increased as total phytoplankton biomass increased, leading up to the bloom maximum. Thus, grazing potential was likely high, and any advantages gained by grazing deterrence could have altered the balance of growth versus grazing in favor of *K. veneficum*. KmTx 2 has been shown to inhibit the feeding and growth of *O. marina* (Adolf et al. 2007). Because susceptibility to karlotoxin is dependent on cell membrane sterol composition and cell membrane sterol compositions vary widely among planktonic organisms (Adolf et al. 2006b), similar grazing deterrence is probable for other micrograzers as well.

For *K. veneficum* (Adolf et al. 2007) and toxic phytoplankton, in general (Sunda et al. 2006), grazing deterrence becomes more effective as the toxic phytoplankton becomes a larger percentage of the total phytoplankton population. However, this positive feedback also implies that grazing deterrence was likely less effective at the beginning of the bloom development when *K. veneficum* was a very small portion of the phytoplankton. This suggests that some other factor or factors may also have been important for selecting *K. veneficum*.

One possibility is the enhanced growth potential of *K. veneficum* when it is feeding mixotrophically. Laboratory studies have shown that mixotrophy can enhance intrinsic growth rates of *K. veneficum* two- to threefold compared to autotrophic growth alone (Li et al. 1999; Adolf et al. 2006a). Small cryptophytes, a preferred prey item of *K. veneficum* (Li et al. 2000), were abundant (~2,000 cells per milliliter) during bloom development (Table 2), indicating the potential for significant mixotrophic growth enhancement. Most of the other dinoflagellates common during the bloom period are also known mixotrophs (Jeong et al. 2005). However, the karlotoxins produced by *K. veneficum* are known to immobilize prey before capture (Li et al. 1999; Adolf et al. 2006b), thereby, increasing mixotrophic feeding efficiency relative to other dinoflagellates (Adolf et al. 2006b). Thus, the initial importance of karlotoxin production in *K. veneficum* bloom development may be growth enhancement rather than grazing deterrence.

The chemical form or combination of available nutrients may also have selected for *K. veneficum*. Kempton et al. (2002) noted that *K. veneficum* blooms in several brackish water ponds were coincident with high NH_4^+ concentrations. Perhaps, the high NH_4^+ availability early during bloom development favored *K. veneficum*. Glibert et al. (2001) suggested that high levels of dissolved organic matter may select for HAB species. However, in this study, the anomalously high concentrations of DON and PO_4^{-3} observed at the biomass maximum on 19 October 2006 were probably not responsible for stimulating *K. veneficum*. Instead, the origin of the excess DON and PO_4^{-3}, which represented 12–13% of the N and P contained in the phytoplankton, was most likely the bloom itself. Accumulation of dissolved organics and PO_4^{-3} because of grazing, cell lysis, or exudation has been shown to occur as dinoflagellate blooms senesce (Holmes et al. 1967). Given the high nutrient demand indicated by low residual DIN (Fig. 7) and enormous phytoplankton biomass at the bloom maximum (Fig. 7), we speculate that, by 19 October 2006, the bloom was near senescence because of nutrient limitation.

Bloom Termination

By 26 October 2006, the dense *K. veneficum* bloom was gone (Fig. 9). The negative apparent growth rates of nearly all phytoplankton species from 19–30 October show that conditions had become unsuitable for sustaining a high level of phytoplankton biomass in the bloom region (Table 2). Salinity data over this time period show no evidence of a major washout event (Fig. 5). Declining water temperatures over the period (Fig. 5) probably decreased intrinsic growth rates of the phytoplankton (Raven and Geider 1988) but were not out of the range permissive for *K. veneficum* growth (Nielsen 1996).

The disproportionate decrease in the abundance of dinoflagellates (Table 2), including *K. veneficum*, suggests that environmental conditions were less favorable for dinoflagellates compared to other phytoplankton groups. Assuming that the cause of the *K. veneficum* collapse was the same as for the other dinoflagellate species, this would generally rule out infectious agents because most pathogens and parasites display a fair degree of host specificity (Park et al. 2004). It also seems unlikely that grazing would so disproportionately affect dinoflagellates, although some tintinnids are known to preferentially feed on dinoflagellates (Stoecker et al. 1981).

A more likely explanation for the catastrophic collapse of dinoflagellate biomass is that small-scale shear associated with the wind mixing event on 20–21 October 2006 (Fig. 5) caused physiological or structural damage to dinoflagellate cells. Dinoflagellates are generally considered the most shear-sensitive of the phytoplankton classes and display growth inhibition or mortality at shear stress levels that are orders of magnitude lower than other phytoplankton (Juhl et al. 2000). The impact of shear may have been exacerbated by its growth stage if, as the accumulation of DON and PO_4^{-3} at the bloom maximum (Fig. 7) suggests, the bulk of the bloom biomass was in its senescent phase (Juhl et al. 2000).

Association with Fish Kills

The fish kills were closely coincidental, temporally and spatially, with the declining *K. veneficum* bloom. We postulate that the strong wind mixing event on 20–21

October 2006 caused sufficient turbulence to disrupt the *K. veneficum* bloom that was already in a senescent phase. Because of the initial strong south wind (Fig. 5), senescent cells and any toxin released from these cells would likely have been carried from the bloom area northward toward the affected creeks (Luettich, R. A. Jr., personal communication). Dissolved KmTx 2 retains toxic activity for up to 2 days (Deeds et al. 2002), allowing ample opportunity for lethal exposure to the fish in the affected creeks. Furthermore, sampling by NCDENR showed *K. veneficum* was present in creek waters (Table 4) where fish were actively dying, although at levels lower than the 15,000 cells per milliliter normally required to kill fish (Deeds et al. 2002). The declining *K. veneficum* cell concentrations between the earliest fish kill reports and the fish kills reported ~1 week later (Table 4) were consistent with the declining cell numbers observed in the main stem of the NRE (Table 2), indicating the likelihood that *K. veneficum* cell densities in the creeks were higher in the days before the fish kills. Senescence and rupture of these cells in these creeks, as well as those being advected into the region from the central part of the estuary, are postulated to have released sufficient toxin to cause the fish kills. Similarly, at a fish farm in Maryland, fish death occurred only after the *K. veneficum* bloom was terminated by addition of copper sulfate (Deeds et al. 2002).

The conclusion that toxins were released from the *K. veneficum* cells is supported by the premortem observation that fish in the affected region were gulping air (Table 4) despite evidence that the water column was fully oxygenated (Table 4; Fig. 5). It is known that the primary ichthyocidal activity of *K. veneficum* toxin is asphyxiation, resulting from damage to gill epithelial cells (Nielsen 1993; Deeds et al. 2006). Juvenile cod (*Gadus morhua*; Nielsen 1993) and red drum (*Sciaenops ocellatus*; Deeds et al. 2002) exposed to high densities of *K. veneficum* have been shown to gulp air at the surface and to show disoriented swimming patterns before death. Both behaviors are consistent with a general response to blood hypoxia in fish (Kramer 1987).

Conclusion

The *K. veneficum* bloom described in this manuscript underscores the tight control of HABs by meteorological forcing, estuarine hydrology, and sediment nutrient input in this shallow lagoonal estuary. Runoff after Tropical Storm Ernesto initially resulted in increased flushing and low algal biomass, as has been found for prior tropical storms (Peierls et al. 2003). As riverine discharge declined, estuarine circulation and low-wind stress resulted in a prolonged period of intense vertical stratification. This stratification was associated with hypoxic bottom water and the accumulation of NH_4^+ and PO_4^{-3} to levels rarely observed in the Neuse River Estuary. A brief wind event mixed the regenerated nutrients throughout the water column. This mixing event was followed by nearly 2 weeks of moderate stratification and stable flushing rates. Nutrient, salinity, light, temperature, and hydrologic conditions during this period were all favorable for phytoplankton growth.

The result was a large bloom that became dominated by dinoflagellates, in part caused by their ability to vertically migrate over the shallow stratified water column to acquire light and additional nutrients as needed. Vertical migration further allowed the physical concentration of dinoflagellates in the bloom region because of the prevailing frontal zone circulation pattern. We speculate that grazing deterrence and enhancing mixotrophic nutrition because of toxin production by *K. veneficum* allowed it to out compete other potential bloom-forming dinoflagellates (Adolf et al. 2006b, 2007). Similar growth advantages associated with toxin production have been postulated to account for the success of other HAB species (Sunda et al. 2006). Bloom termination was probably caused by the disruption of an already-senescing population by a turbulent-wind mixing event. Toxin released during bloom termination was postulated to be the cause of subsequent fish kills. The conditions leading to HAB formation are typically short lived and difficult to measure at appropriate spatial and temporal scales for assessing bloom dynamics (Fogg 2002). Our ability to infer some of the factors leading to this bloom was only possible because of the combined data from ModMon, USGS, NC DENR–DWQ, and CASTNET monitoring programs. Such networks are crucial for advancement in understanding HAB dynamics.

Acknowledgment Thanks to the dedicated technicians of the Paerl, Litaker (Mark W. Vandersea), and Place laboratories for their analytical contributions. Thanks to A. Joyner for help in generating the site map. R. Waggett, B. Peierls, and W. G. Sunda provided constructive critiques of the manuscript. This work was supported by the North Carolina Department of Environment and Natural Resources (ModMon Program), the North Carolina Sea Grant Program, the US EPA-STAR-EaGLe Program, and the National Science Foundation, Ecosystems, Environmental Geochemistry and Biology (EGB) and Ecology of Infectious Diseases (EID) Programs. Toxin analyses were supported by grants from NOAA Coastal Oceans Program (grant no. NA04NOS4780276), Centers for Disease Control and Prevention (grant no. U50/CCU 323376) and the Maryland Department of Health and Mental Hygiene to University of Marine Biotechnology Institute. This is contribution number 220 from the NOAA ECOHAB program and contribution number 07-172 from the University of Maryland Biotechnology Institute, Center of Marine Biotechnology.

References

Adolf, J.E., D.K. Stoecker, and L.W. Harding Jr. 2003. Autotrophic growth and photoacclimation in *Karlodinium micrum* (dinophy-

ceae) and *Storeatula major* (cryptophyceae). *Journal of Phycology* 39: 1101–1108.

Adolf, J.E., D.K. Stoecker, and L.W. Harding Jr. 2006a. The balance of autotrophy and heterotrophy during the mixotrophic growth of *Karlodinium micrum* (Dinophyceae). *Journal of Plankton Research* 28: 737–751.

Adolf, J.E., T.R. Bachvaroff, D.N. Krupatkina, H. Nonogaki, P.J.P. Brown, A.J. Lewitus, H.R. Harvey, and A.R. Place. 2006b. Species specificity and potential roles of *Karlodinium micrum* toxin. *African Journal of Marine Science* 28: 415–419.

Adolf, J.E., T.R. Bachvaroff, D.N. Krupatkina, and A.R. Place. 2007. Karlotoxin mediates grazing by *Oxyrrhis marina* on strains of *Karlodinium veneficum*. *Harmful Algae* 6: 400–412.

Amano, K., M. Watanabe, K. Kohata, and S. Harada. 1998. Conditions necessary for *Chattonella antiqua* red tide outbreaks. *Limnology and Oceanography* 43: 117–128.

Ault, T.R. 2000. Vertical migration by the marine dinoflagellate *Prorocentrum triestinum* maximizes photosynthetic yield. *Oecologia* 125: 266–475.

Bachvarroff, T.R., J.E. Adolf, A. Squier, H.R. Harvey, and A.R. Place. 2007. Characterization and quantification of karlotoxins by liquid chromatography–mass spectrometry. *Harmful Algae* (IN PRESS). DOI 10.1016/j.hal.2007.10.003.

Bowers, H.A., C. Tomas, J.W. Kempton, A.J. Lewitus, T. Tengs, and D.W. Oldach. 2006. Raphidophyceae [Chadefaud ex Silva] systematics and rapid identification: sequence analyses and real-time PCR assays. *Journal of Phycology* 42: 1333–1348.

Campbell, P.H. 1973. *Studies on brackish water phytoplankton*. Chapel Hill, North Carolina: University of North Carolina Sea Grant Program.

Chang, J., and E.J. Carpenter. 1985. Blooms of the dinoflagellate *Gyrodinium aureolum* in a Long Island estuary: box model analysis of bloom maintenance. *Marine Biology* 89: 83–93.

Clesceri, L.S., A.E. Greenberg, and A.D. Eaton (eds.). 1998. *Standard methods for the examination of water and wastewater*, 20th edn, 10–13, 1. Washington, DC: American Public Health Association.

Cloern, J.E. 2001. Our evolving conceptual model of the coastal eutrophication problem. *Marine Ecology Progress Series* 210: 223–253.

Cloern, J.E., T.S. Schraga, C.B. Lopez, N. Knowles, R.G. Labiosa, and R. Dugdale. 2005. Climate anomalies generate an exceptional dinoflagellate bloom in San Francisco Bay. *Geophysical Research Letters* 32: L14608.

Daugbjerg, N., G. Hansen, J. Larsen, and O. Moestrup. 2000. Phylogeny of some of the major genera of dinoflagellates based on ultrastructure and partial LSU rDNA sequence data, including the erection of three new genera of unarmoured dinoflagellates. *Phycologia* 39: 302–417.

Deeds, J.R., D.E. Terlizzi, J.E. Adolf, D.K. Stoecker, and A.R. Place. 2002. Toxic activity from cultures of *Karlodinium micrum* (=*Gyrodinium galatheanum*) (Dinophyceae) a dinoflagellate associated with fish mortalities in an estuarine aquaculture facility. *Harmful Algae* 1: 169–189.

Deeds, J.R., R. Reimschussel, and A.R. Place. 2006. Histopathological effects in fish exposed to the toxins from *Karlodinium micrum* (Dinophyceae). *Journal of Aquatic Animal Health* 18: 136–148.

Eschbach, E., J. Scharsack, U. John, and L. Medlin. 2001. Improved erythrocyte lysis assay in microtitre plates for sensitive detection and efficient measurement of haemolytic compounds from ichthyotoxic algae. *Journal of Applied Toxicology* 21: 513–539.

Fensin, E.E. 2004. Occurrence and ecology of the dinoflagellate *Karlodinium micrum* in estuaries of North Carolina, USA. In *Harmful algae 2002*, eds. K.A. Steidinger, J.H. Landsberg, C.R. Tomas, and G.A. Vargo, 62–67. St. Petersburg, FL: Florida Fish and Wildlife Conservation Commission, Florida Institute of Oceanography, and Intergovernmental Oceanographic Commission of UNESCO.

Fogg, G.E. 2002. Harmful algae—a perspective. *Harmful Algae* 1: 1–4.

Glibert, P.M., R. Magnien, M.W. Lomas, J. Alexander, C. Fan, E. Haramoto, M. Trice, and T.M. Kana. 2001. Harmful algal blooms in the Chesapeake and coastal bays of Maryland, USA: comparison of 1997, 1998, and 1999 events. *Estuaries* 24: 875–883.

Goshorn, D., J. Deeds, P. Tango, C. Poukish, A. Place, M. McGinty, W. Butler, C. Luckett, and R. Morgan. 2004. Occurrence of *Karlodinium micrum* and its association with fish kills in Maryland estuaries. In *Harmful Algae 2002*, eds. K.A. Steidinger, J.H. Landsberg, C.R. Tomas, and G.A. Vargo, 361–363. St. Petersburg, FL: Florida Fish and Wildlife Conservation Commission, Florida Institute of Oceanography, and Intergovernmental Oceanographic Commission of UNESCO.

Hallegraeff, G.M. 1993. A review of harmful algal blooms and their apparent global increase. *Phycologia* 32: 79–99.

Hansen, B., P.K. Bjornsen, and P.J. Hansen. 1994. The size ratio of planktonic predators and their prey. *Limnology and Oceanography* 39: 395–403.

Holmes, R.W., P.M. Williams, and R.W. Eppley. 1967. Red water in La Jolla Bay, 1964–1966. *Limnology and Oceanography* 12: 503–512.

Janowitz, G.S., and D. Kamykowski. 2006. Modeled *Karenia brevis* accumulation in the vicinity of a coastal nutrient front. *Marine Ecology Progress Series* 314: 49–59.

Jeong, H.J., D.Y. Yeong, J.Y. Park, J.Y. Song, S.T. Kim, S.H. Lee, K.Y. Kim, and W.H. Yih. 2005. Feeding by phototrophic red-tide dinoflagellates: five species newly revealed and six species previously known to be mixotrophic. *Aquatic Microbial Ecology* 40: 133–150.

Johnson, M.D., M. Rome, and D.K. Stoecker. 2003. Microzooplankton grazing on *Prorocentrum minimum* and *Karlodinium micrum* in Chesapeake Bay. *Limnology and Oceanography* 48: 238–248.

Juhl, A.R., V. Velazquez, and M.I. Latz. 2000. Effect of growth conditions on flow-induced inhibition of population growth of a red-tide dinoflagellate. *Limnology and Oceanography* 45: 905–915.

Kempton, J.W., A.J. Lewitus, J.R. Deeds, J.M. Law, and A.R. Place. 2002. Toxicity of *Karlodinium micrum* (Dinophyceae) associated with a fish kill in a South Carolina brackish retention pond. *Harmful Algae* 1: 233–244.

Kramer, D.L. 1987. Dissolved oxygen and fish behaviour. *Environmental Biology of Fishes* 18: 81–92.

Li, A., D.K. Stoecker, and J.E. Adolf. 1999. Feeding, pigmentation, photosynthesis and growth of the mixotrophic dinoflagellate *Gyrodinium galatheanum*. *Aquatic Microbial Ecology* 19: 163–176.

Li, A., D.K. Stoecker, and D.W. Coats. 2000. Spatial and temporal aspects of *Gyrodinium galatheanum* in Chesapeake Bay: distribution and mixotrophy. *Journal of Plankton Research* 22: 2105–2124.

Luettich, R.A., J.E. McNinch, H.W. Paerl, C.H. Peterson, J.T. Wells, M.A. Alperin, C.S. Martens, and J.L. Pinckney. 2000. *Neuse River Estuary modeling and monitoring project stage 1: hydrography and circulation, water column nutrients and productivity, sedimentary processes and benthic–pelagic coupling, and benthic ecology*. North Carolina: North Carolina Water Resources Research Institute Report 325 B. Raleigh.

Luettich, R.A., S.D. Carr, and J.V. Reynolds-Fleming. 2002. Semidiurnal seiching in a shallow, micro-tidal lagoonal estuary. *Continental Shelf Research* 22: 1669–1681.

Miller, W.D., L.W. Harding, and J.E. Adolf. 2006. Hurricane Isabel generated an unusual fall bloom in Chesapeake Bay. *Geophysical Research Letters* 33: L06612.

Nakamura, Y., S. Suzuki, and J. Hiromi. 1996. Development and collapse of a *Gymnodinium mikimotoi* red tide in the Seto Inland Sea. *Aquatic Microbial Ecology* 10: 131–137.

Nielsen, M.V. 1993. Toxic effects of the marine dinoflagellate *Gymnodinium galatheanum* on juvenile cod *Gadus morhua*. *Marine Ecology Progress Series* 95: 273–277.

Nielsen, M.V. 1996. Growth and chemical composition of the toxic dinoflagellate *Gymnodinium galatheanum* in relation to irradiance, temperature, and salinity. *Marine Ecology Progress Series* 136: 205–211.

North Carolina Department of Environment and Natural Resources—Division of Water Quality. 2001. Phase II of the total maximum daily load for total nitrogen to the Neuse River Estuary, North Carolina. Raleigh, North Carolina: NCDENR–DWQ.

North Carolina Department of Environment and Natural Resources—Division of Water Quality. 2007. Environmental Sciences Section. Fish kill data base 2006. http://h2o.enr.state.nc.us/esb/Fishkill/fishkillmain.htm. Accessed 6 June 2007.

Paerl, H.W., J.L. Pinckney, J.M. Fear, and B.L. Peierls. 1998. Ecosystem responses to internal and watershed organic matter loading: consequences for hypoxia in the eutrophying Neuse River Estuary, North Carolina, USA. *Marine Ecology Progress Series* 166: 17–25.

Paerl, H.W., L.M. Valdes, M.F. Piehler, and M.E. Lebo. 2004. Solving problems resulting from solutions: The evolution of a dual nutrient management strategy for the eutrophying Neuse River Estuary, North Carolina, USA. *Environmental Science & Technology* 38: 3068–3073.

Park, M.G., W. Yih, and D.W. Coats. 2004. Parasites and phytoplankton, with special emphasis on dinoflagellate infections. *Journal of Eukaryotic Microbiology* 51: 145–155.

Peierls, B.L., R.R. Christian, and H.W. Paerl. 2003. Water quality and phytoplankton as indicators of hurricane impacts on a large estuarine ecosystem. *Estuaries* 26: 1329–1343.

Pinckney, J.L., D.F. Millie, K.E. Howe, H.W. Paerl, and J.P. Hurley. 1996. Flow scintillation counting of ^{14}C-labeled microalgal photosynthetic pigments. *Journal of Plankton Research* 18: 1867–1880.

Pinckney, J.L., D.F. Millie, B.T. Vinyard, and H.W. Paerl. 1997. Environmental controls of phytoplankton bloom dynamics in the Neuse River Estuary, North Carolina, USA. *Canadian Journal of Fisheries and Aquatic Sciences* 54: 2491–2501.

Raven, J.A., and R.J. Geider. 1988. Temperature and algal growth. *New Phytologist* 110: 441–461.

Smayda, T.J. 1997. Harmful algal blooms: Their ecophysiology and general relevance to phytoplankton blooms in the sea. *Limnology and Oceanography* 42: 1137–1153.

Steidinger, K.A. 1983. A re-evaluation of toxic dinoflagellate biology and ecology. *Progress in Phycological Research* 2: 147–188.

Stoecker, D., R.L. Guillard, and R.M. Kavee. 1981. Selective predation by *Favella ehrenbergii* (Tintinnia) on and among dinoflagellates. *Biological Bulletin* 160: 136–145.

Sunda, W.G., E. Graneli, and C.J. Gobler. 2006. Positive feedback and the development and persistence of ecosystem disruptive algal blooms. *Journal of Phycology* 42: 963–974.

Tyler, M.A., and H.H. Seliger. 1978. Annual subsurface transport of a red tide dinoflagellate to its bloom area: Water circulation patterns and organism distributions in the Chesapeake Bay. *Limnology and Oceanography* 23: 227–246.

Utermöhl, H. 1958. Zur Vervollkommnung der quantitativen phytoplanktonmethodik. *Mitteilungen, Internationale Vereinigung fr Theoretische und Angewandte Limnologie* 9: 1–38.

Valdes-Weaver, L.M., M.F. Piehler, J.L. Pinckney, K.E. Howe, K. Rosignol, and H.W. Paerl. 2006. Long-term temporal and spatial trends in phytoplankton biomass and class-level taxonomic composition in the hydrologically variable Neuse–Pamlico estuarine continuum, NC, USA. *Limnology and Oceanography* 51: 1410–1420.

Vollenweider, R.A. 1974. *A manual for measuring primary production in aquatic environments. IBP handbook no. 12. F. A*. Philadelphia: Davis Company.

Waggener, A.L. 2006. The chlorophyll—a maximum of the Neuse River Estuary, North Carolina, United States of America: Nutrient dynamics and trophic interaction at the most productive region of the system. North Carolina. M.S. thesis, University of North Carolina at Chapel Hill.

Watras, C.J., V.C. Garcon, R.J. Olson, S.W. Chisholm, and D.M. Anderson. 1985. The effect of zooplankton grazing on estuarine blooms of the toxic dinoflagellate *Gonyaulax tamarensis*. *Journal of Plankton Research* 7: 891–908.